Composites Science and Technology 214 (2021) 108982

Contents lists available at ScienceDirect

Composites Science and Technology

journal homepage: www.elsevier.com/locate/compscitech

Dehydrofluorinated PVDF for structural health monitoring in fiber reinforced composites

LoriAnne Groo [a], Daniel J. Inman [a], Henry A. Sodano [a,b,c,*]

[a] Department of Aerospace Engineering, University of Michigan, Ann Arbor, MI, 48109, United States
[b] Department of Macromolecular Science and Engineering, University of Michigan, Ann Arbor, MI, 48109, United States
[c] Department of Materials Science and Engineering, University of Michigan, Ann Arbor, MI, 48109, United States

ARTICLE INFO

Keywords:
Polymer composites
Smart materials
Piezoelectric sensing
Structural health monitoring
Multifunctional composites

ABSTRACT

Structural health monitoring of fiber reinforced composites is an extensive field of research that aims to reduce maintenance costs through in-situ damage detection. However, the need for externally bonded sensor systems and complicated fabrication processes limit the widespread application of most current structural health monitoring techniques. This work introduces a novel multifunctional fiber reinforced composite that relies on a ferroelectric prepreg fabricated using dehydrofluorinated (DHF) polyvinylidene fluoride (PVDF), which exhibits a thermally stable piezoelectric response. The self-sensing material presented in this work requires minimal external components, as the piezoelectric sensing mechanism is fully contained within the composite. This is accomplished by fabricating a ferroelectric prepreg consisting of DHF PVDF infused woven fiberglass, which is sandwiched between woven carbon fabric layers that act as electrodes, thus forming a piezoelectric sensor fabricated with entirely structural composite materials. Notably, the sensing material is a fully distributed prepreg rather than discretely embedded sensors which enables simplified monitoring of complex structures. As the composite experiences damage under flexural and tensile loading, the internal change in strain results in a charge separation that is detectable as a voltage emission across the sample electrodes. The self-sensing capabilities of this material are explored using traditional mechanical testing techniques, showing comparable performance to common damage detection methods, all while eliminating the need for external bonding of sensors to the structure.

1. Introduction

Fiber reinforced polymer matrix composites play a crucial role in several industrial applications due to their high strength to weight ratio and the capability to tailor directional properties, allowing for greater flexibility during design. As a result, composites are exposed to complex loading scenarios in aircraft, automobiles, and boats, which all take advantage of the low density of the composite material to achieve a higher performance at reduced cost. To maintain high performance and structural safety, these materials are periodically inspected to search for the existence of damage such as matrix cracking, fiber failure, debonding between fiber and matrix, or delamination between plies. Due to the critical nature of structural materials, damage requires early diagnosis and analysis in order to avoid propagation, which can lead to catastrophic failure. As an alternative to periodic removal of the structures from service, extensive interest has been placed towards structural health monitoring (SHM) of composite materials using multiple in-situ monitoring methods such as acoustic emission testing (AET) [1–4], resistance-based monitoring [5–9], and fiber optic sensors [10–13]. Specifically, in-situ monitoring of composite materials has the potential to provide continuous assessment of the damage state of the material, thus increasing the safety of the structure and reducing the cost of maintenance by eliminating the need to remove the structure from service.

Among the various in-situ monitoring techniques, resistance-based damage sensing uses the inherent composite properties to detect damage as it occurs [5–7]. This methodology relies on conductive pathways formed either by conductive fiber reinforcement, typically in the form of carbon fibers [5,6,14–17], or added conductive fillers, such as graphene oxide [18,19] or carbon nanotubes (CNTs) [9,20–23]. As damage occurs within the composite, separation occurs within some of the conductive (carbon-carbon) contacts, thus resulting in a corresponding increase in

* Corresponding author. Department of Aerospace Engineering, University of Michigan, Ann Arbor, MI, 48109, United States.
E-mail address: hsodano@umich.edu (H.A. Sodano).

https://doi.org/10.1016/j.compscitech.2021.108982
Received 6 October 2020; Received in revised form 12 July 2021; Accepted 4 August 2021
Available online 8 August 2021

electrical impedance. CNTs have gained traction in this particular application due to their multifunctional properties which contribute to strengthening of the composite while also introducing piezoresistivity to electrically insulating composites utilizing reinforcements such as glass or aramid fibers [20,24,25]. However, it is well-known that CNTs are difficult to evenly disperse in common matrix materials due to their tendency to agglomerate as a result of van der Waals forces, which complicates their ability to achieve the required distribution for the large-scale application of embedded composite strain monitoring [26,27]. Additionally, resistance-based monitoring techniques require a constant power input to continually monitor the state of the structure, thus inherently necessitating power to assess large structures or small structures over long periods of time.

Alternatively, fiber optic sensors have been widely studied since they can be embedded directly into the fiber reinforced composite material during fabrication, and can sense strain as well as damage [10,11,28–31]. These fiber sensors are able to use changes in optical properties, such as intensity, wavelength, phase, etc., in response to mechanical strain. These changes can then be correlated to a damage or changing structural state [10]. In addition, fiber Bragg grating (FBG) sensors can also be used for ultrasonic acoustic emission testing (AET) [32–34], however, due to the discrete nature of the fiber sensors, the embedded fibers require specific orientation and placement relative to the damage location for accurate sensing [35,36]. Traditionally, rather than using FBG sensors, AET typically relies on piezoelectric materials that are either externally bonded to or embedded within the composite structure of interest [1,2,37–40]. As damage occurs within the material, a corresponding release of energy results in a propagating wave that can be sensed by the piezoelectric sensors close to the damage source as they can convert the mechanical energy to a measurable electrical signal via the direct piezoelectric effect. Due to its flexibility and conformability when attached to the surface of materials and its less invasive presence when embedded within materials, PVDF in the form of film sensors has received considerable interest for AET sensing [41–44]. However, current PVDF sensors used for AET require discrete embedding within the composite or external attachment, thus isolating the damage sensing to a limited area or requiring large networks of sensors for monitoring of larger structures. Thus, an alternative to discrete and external PVDF sensors is required for the efficient damage monitoring of industrial-scale structures.

PVDF is an appealing piezoelectric material as it possesses the flexibility of a polymer in addition to strong piezoelectric coupling, and, as such, is easily conformable for various sensing and actuating applications [45–49]. PVDF crystallizes in three different phases, the amorphous α-phase, the partial polarity γ-phase, and the polar β-phase [50–52]. For piezoelectric applications, the β-phase is the most desirable phase as it results in the highest piezoelectric, ferroelectric, and pyroelectric properties [51–53]. For this reason, increasing the fraction of β-phase in PVDF has been a topic of interest over many years. Among the methods investigated, uniaxial drawing is the most commonly used to mechanically align the polymer chains in a parallel orientation and form planar conformation, or β-phase [54–56]. However, since drawn PVDF relies on the physical shape of the polymer, thermal relaxation occurs at elevated temperatures above the Curie temperature of the PVDF, resulting in a return to the energy-preferential amorphous α-phase, thus reducing or eliminating the piezoelectric response [57,58]. In contrast to mechanically drawn PVDF, dehydrofluorinated (DHF) PVDF produces the energy-preferential formation of a thermally stable electroactive β- and γ-phases [59]. The dehydrofluorination process is referred to as the chemical reaction, which takes place when PVDF is exposed to a basic environment, resulting in a loss of the hydrogen fluoride (HF) molecule, and leading to carbon-carbon double bonds in the backbone of the PVDF. The extent of dehydrofluorination can thus be controlled by adjusting the basicity of the environment and the exposure duration to achieve preferential levels of β- γ-and phases. Since the induced electroactive phases are the product of a chemical adjustment to traditional PVDF, it exhibits thermal stability up to ~200 °C which is notably superior to drawn PVDF [59].

This work combines the benefits of resistance-based monitoring and the piezoelectric sensing methodology of AET using thermally stable DHF PVDF to self-sense composite damage in-situ. The multifunctional material described here uses ferroelectric DHF PVDF that is distributed throughout the structural composite by fabricating a fiberglass prepreg using DHF PVDF. The ferroelectric prepreg is then sandwiched between woven carbon fiber plies which act as electrodes, producing a hybrid composite of similar base components to that of a conventional piezoelectric sensor. The sensing material thus requires no discrete placement or distributed sensor system to detect damage in large structures in contrast to previously investigated embedded PVDF films. Once the composite specimen is subjected to damage, the piezoelectric DHF PVDF undergoes a rapid change in strain resulting in a charge separation that is measured as a sudden voltage emission across the sample. This methodology has been previously described by Groo et al. who utilized piezoelectric zinc oxide (ZnO) nanowires as an integrated sensing material within a hybrid composite formed using ZnO coated aramid fabric sandwiched in between carbon fiber electrodes [60]. Based upon a similar damage detection methodology, this work uses a new method to fabricate a ferroelectric prepreg for use in self-sensing composites, and the sensing capabilities of the resultant hybrid composite are assessed through both three-point bend and tensile tests.

2. Experimental section

2.1. DHF PVDF preparation

The DHF PVDF in this work was fabricated using concepts first explored by Lin et al. [59]. When subjected to basic or high temperature environments, PVDF loses hydrogen fluoride (HF) in a process referred to as dehydrofluorination. In this case, 1,8-diazabicyclo (5.4.0)undec-7-ene (DBU) (98+%, Acros Organics™) was selected as the preferred base due to the relatively moderate rate and controllability of the reaction. Specifically, 0.1 wt% DBU was added to 7 wt% PVDF (Kynar 301F) powder dissolved into N,N-dimethylformamide (DMF) (Certified ACS, Fisher Chemical) and thoroughly mixed. The mixture was then left for 1 h, while the dehydrofluorination reaction progressed. The resulting PVDF mixture was then slowly poured over deionized (DI) water mixed with 1 vol% hydrochloric acid (HCl) (Certified ACS Plus, Fisher Chemical) to terminate the reaction. The precipitated DHF PVDF, which forms as a consequence of the hydrophobicity of PVDF, was simultaneously collected from the fluid surface during the pouring process. The collected DHF PVDF film was then rinsed with additional DI water and HCl, after which it was sonicated in DI water and HCl for 10 min. Following the sonication, the film was thoroughly rinsed with pure DI water and sonicated again in DI water for 10 min. The rinsing and washing process was then repeated three times with ethanol to ensure no DMF or DBU remained trapped in the collected DHF PVDF product. Following the completion of the full cleaning process, the DHF PVDF was thoroughly dried in a convection oven at 55 °C for several hours.

Once the DHF process was completed, 10–15 wt% dried DHF PVDF product was thoroughly dissolved in DMF using shear mixing (Flackteck speedmixer DAC 150.1 FVZ). The DHF PVDF solution was then poured over two stacked layers of S-glass, plain-weave fabric (US Composites Style 6533) and subsequently dried at 80 °C under vacuum for 5–10 h to form a prepreg. Once the DMF was fully evaporated, an additional thin layer of the DHF PVDF solution was added to the prepreg and fully dried under vacuum. This process was repeated several times until the combined DHF PVDF polymer layers reached the same thickness as the woven fiberglass. Following the evaporation of the DMF in the final layer of the matrix, the fiberglass/DHF PVDF prepreg was pressed for 1 h in a hot press at 177 °C (350 °F) and ~100 psi, which is the melting temperature of PVDF, in order to fully and evenly infuse the PVDF matrix through the woven fabric and remove any air pockets. Following pressing of the PVDF into the plain-weave fiberglass fabric, the prepreg was annealed at 180 °C for 20 min in an oven to encourage crystal growth for the formation of the electroactive β- and γ-phases, after which the prepreg was allowed to cool slowly at a rate of ~0.5 °C/min.

2.2. Composite fabrication

The resulting prepreg was then combined with three total plies of plain-weave carbon fiber (Hexcel® Style 282, received from Pacific Coast Composites) and infused with epoxy resin consisting of Epon 862 resin and curing agent Epikure 3230 (both received from Hexion) at a ratio of 100:35. For reference, the resultant epoxy matrix has a Young's modulus of 2.54 ± 0.06 GPa and a tensile strength of 70.3 ± 1.1 MPa, and has been used in previous works investigating multifunctional fiber-reinforced composites [60–62]. A hand layup process was used in order to ensure even epoxy distribution on both sides of the DHF PVDF prepreg, after which the composite layup was cured at 80 °C (167 °F) under vacuum at 100 psi for 6 h. The final stacking sequence for both the three-point bend and tensile testing samples was two layers of carbon fiber, fiberglass and DHF PVDF prepreg, and one layer of carbon fiber. The described configuration allows for the sandwiching of the piezoelectric prepreg between conductive plies of carbon fiber, which act as electrodes in addition to their structural functionality. Additionally, the asymmetric layup results in increased strain in the functional layer due to its location relative to the midline of the composite, thus increasing the piezoelectric response during bending [62]. Following the fabrication of the layups, the test specimens were cut to the dimensions recommended by their respective ASTM standards. The cut flexure and tensile specimens were then polished to remove some carbon fiber at the edges of the sample and eliminate conductive pathways between the top and bottom carbon fiber plies, thus avoiding any conductivity through the thickness. As is recommended in ASTM standard D3039, fiberglass tabs were added to the ends of the tensile specimens using high shear strength epoxy (Loctite® 9430™ Hysol®). Additionally, a small section of the outer matrix layer was removed from the samples, and wire leads (33-gauge copper wire) were attached close to the end of the test specimens using a combination of silver paint and quick-cure epoxy, enabling voltage measurements across the thickness of the sample without mechanically interfering with the testing. Finally, the samples containing DHF PVDF were directly poled in silicon oil at 1.2 MV/m and 150 °C for 1 h. It can be noted that the electric field used was lower than typically applied for piezoelectric polymers. This is due to the increased risk of shorting due to the fibrous nature of the carbon fiber layers used as electrodes, which can cause bridging of the electrodes. However, the samples exhibited sufficient piezoelectric response at this lower voltage as will be discussed in later sections. A schematic of the fabrication progress is depicted in Fig. 1. It can also be noted that the replacement of a portion of the composite matrix with DHF PVDF resulted in maintained mechanical properties within the interlaminar region when the prepreg was strategically placed at an offset location as confirmed through short beam shear (SBS) testing (Fig. S1).

2.3. Three-point bend testing

To investigate the in-situ flexural damage detection properties of the samples with DHF PVDF, three-point bend testing following ASTM standard D7264 was completed using an Instron Model 5982 load frame with a 100 kN load cell. The 1.05 mm thick samples were cut to a width of approximately 13 mm and a length of approximately 100 mm as is recommended by the standard. It can be noted that the thickness and width were measured at the maximum points since the samples did not have a uniform cross-section due to the polishing of the edges. The length of the test specimens is slightly longer than that suggested in the ASTM standard for the purpose of allowing extra surface area for the attachment of the wire leads outside of the testing span. In this configuration, the voltage across the thickness of the sample can be measured throughout the duration of the test without interfering with the mechanical testing. The test specimens were tested at a span to thickness ratio of 32:1 to ensure significant damage would occur within a reasonable time frame and sample extension. It should also be noted that non-conductive Kapton® tape was placed at the contact points of the test setup to eliminate any electrical interference between the test frame and the test specimen. The voltage across the sample was measured for the duration of each test across the outer plies of carbon fiber using a National Instruments (NI) 4431 data acquisition system (DAQ). Additionally, a high frequency microphone (PCB 426A05) in combination with a PCB 482A16 signal conditioner was used to detect acoustic emissions in order to validate the occurrence of damage during the test. A 20 kHz Butterworth second order high pass filter was applied to the microphone readings to remove unwanted noise from the measurement. To confirm the role of the DHF PVDF in damage detection, neat composite specimens fabricated using the same layup configuration (0.92 mm thickness) and solely infused with epoxy were also tested using the same setup for comparison.

2.4. Tensile testing

In addition to sensing during flexural loading, the capacity of the

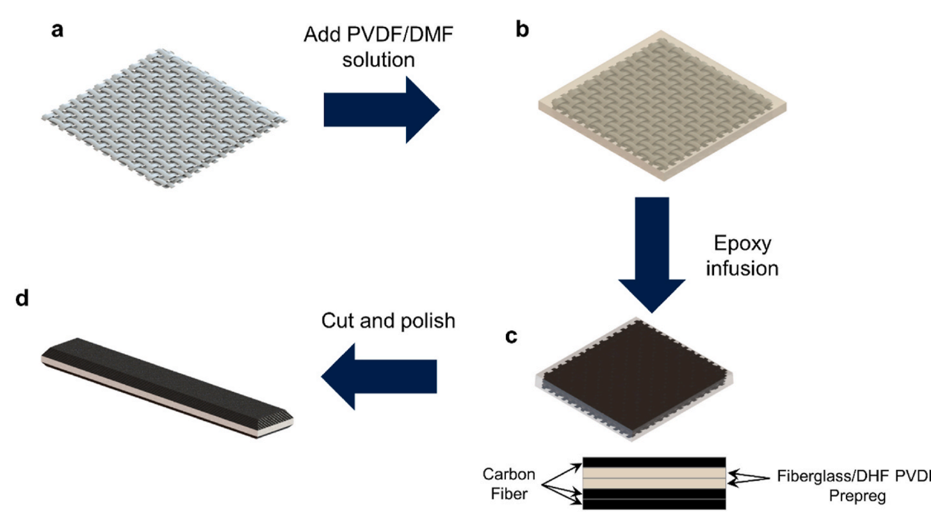

Fig. 1. Schematic of (a) two plies of neat plain weave fiberglass, (b) fiberglass infused with PVDF, (c) final composite comprised of two layers of carbon fiber, fiberglass with PVDF, and one layer of carbon fiber with an epoxy matrix, and (d) final cut and polished sample.

samples to detect damage during tensile loading was also assessed. To achieve this, the samples were loaded in a tensile test per ASTM standard D3039 using the same Instron Model 5982 load frame with a 100 kN load cell. The samples were cut to dimensions of approximately 13 mm in width and 100 mm in length, resulting in a gauge length of ~75 mm. The fiberglass tabs attached to the ends of each composite sample served a dual purpose as they both prevented slipping of the composite beams or samples and acted as an electrically insulating barrier between the composite sample and the test frame. As with the flexural testing, the voltage across the thickness of the sample was monitored throughout the duration of the tests. Additionally, the same high frequency microphone and signal conditioner were once again used to confirm the damage via acoustic emissions. To establish necessity of the DHF PVDF for damage sensing, neat composite samples fabricated using a similar stacking layup, and without the DHF PVDF component, were tested as a basis for comparison.

3. Results and discussion

3.1. DHF PVDF characterization

The merit of the dehydrofluorination process lies in the concept that the formation of C═C bonds in the polymer backbone lead to rotational stiffness which induces formation of the β-phase rather than the normally thermodynamically stable α-phase [59]. This significant adjustment to the structure of the PVDF affects the preferred phase and results in increased crystallinity, primarily in the form of β-phase. To investigate the phase composition of the DHF PVDF at each stage of the fabrication process in this work and ensure the ferroelectric properties, Fourier-transform infrared spectroscopy (FTIR) was performed following the initial infusion, pressing, and annealing steps. It can be noted that the chemical composition and piezoelectric response of DHF PVDF are fully reported in the reference literature [59], thus FTIR was considered to be sufficient for the purposes of this work when investigating the phase composition of the DHF PVDF prepreg. The resulting spectra taken after each step can be seen in Fig. 2 with the baseline measurement representing the prepreg following initial infusion. It can be noted that the spectra were taken directly from the surface of the prepreg, and the prepreg received no additional treatment prior to the measurements. It is clear from the figure that the initial combination of the PVDF with the fiberglass fabrics results in the formation of primarily (β+γ)-phase PVDF as this is the preferred configuration. However,

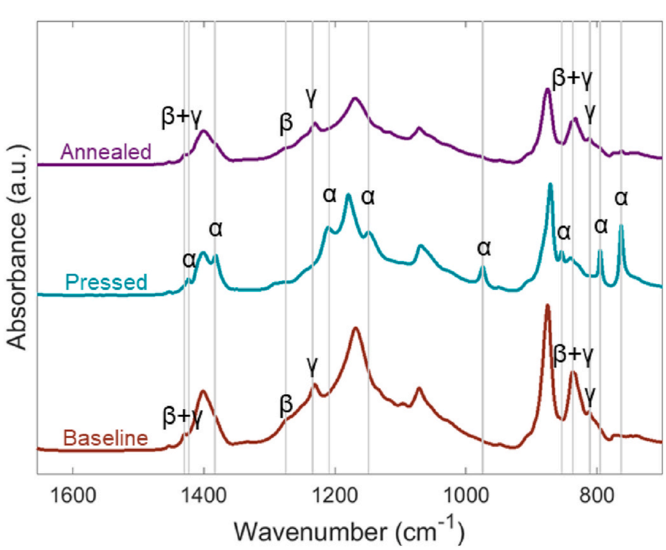

Fig. 2. FTIR spectra of neat DHF PVDF after initial infusion (baseline), pressed DHF PVDF (pressed), and pressed DHF PVDF following the annealing process (annealed).

following the hot press treatment which fully infuses the PVDF into the woven fiberglass, the PVDF is found to be comprised of primarily α-phase. Since DHF PVDF has previously been shown to maintain β-phase in temperatures up to ~210 °C, which is well above the temperature of the hot press step [59], it is assumed that this transition to α-phase under heat and pressure is a result of the flow of the polymer into the fabric and the interaction with the high surface area of the glass resulting in greater confinement, physically limiting the crystal growth of the PVDF that is required to form γ- or β-phase. To encourage crystal growth and thus reintroduce additional ferroelectric potential, the pressed prepreg was annealed at 180 °C in an oven for 20 min and cooled slowly in the same oven so as not to quench crystal growth. As seen in Fig. 2, the resulting annealed surface shows an increase in the peaks corresponding to both γ-phase (811 cm^{-1} and 1234 cm^{-1} wavenumbers) and β-phase (1275 cm^{-1} wavenumber) or a combination (837 cm^{-1} and 1430 cm^{-1} wavenumbers) [63]. For the purpose of this work, the combination of both γ-phase and β-phase was considered to be preferential as both phases result in adequate piezoelectric coupling for damage detection.

3.2. In-situ sensing during three-point bend testing

Both neat hybrid composites and hybrid composites fabricated using DHF PVDF were tested in three-point bend testing to establish the ability of the samples to sense damage resulting from flexural loading. Throughout the duration of the test, the applied stress and resulting voltage across the thickness of the sample were recorded. In addition, the resulting acoustic emission output was measured using a high frequency microphone. Sudden drops in the applied stress that also corresponded to burst signals detected using the high frequency microphone indicated the occurrence of damage. As damage occurs within the loaded composite specimen, a corresponding release of mechanical strain energy results in a propagating elastic wave that was detected via the high frequency microphone. It can be noted that airborne acoustics have been shown to be effective in detecting damage independently [64], and the validity of the methodology was further confirmed here through the correlation between changes to the stress curve and microphone acoustic emission measurements. Fig. 3a–c shows the applied stress, corresponding microphone pressure reading, and voltage across the specimen, respectively, for a neat composite sample during flexural loading. For clarity, the stress and microphone pressure reading during the latter portion of the test (final ~30 %), where the sample experienced significant detectable damage, is shown at a higher magnification in Fig. 3d and e, respectively. From Fig. 3d and e, the previously described evidence of damage occurrence is manifest by the sudden changes in the slope of the stress curve, visually shown as drops in the applied stress, which correspond to bursts in the microphone pressure readings. In contrast to active stress and pressure measurements, the voltage across the representative neat sample is observed to remain relatively constant with little variation in the signal, thus indicating no piezoelectric activity or response to damage. Therefore, the baseline neat hybrid composite samples prove unable to detect damage using voltage measurements.

As a comparison, the applied stress, microphone pressure reading, and voltage across the thickness of a sample containing DHF PVDF are shown in Fig. 4a–c, respectively. As before, the occurrence of damage is observed by drops in the applied stress corresponding to acoustic emission burst measurements from the high frequency microphone. However, in contrast to the neat samples, the voltage measurements across the composite samples containing DHF PVDF showed a response correlating to damage. Fig. 4d and e shows the microphone pressure reading and voltage across the sample, respectively, during the latter portion of the test when the damage is observed to occur (final ~25%). From Fig. 4e, the sample containing DHF PVDF exhibits a voltage emission as a result of the piezoelectric coupling of the DHF PVDF, thus confirming that the combined (β+γ)-phases resulting from the DHF

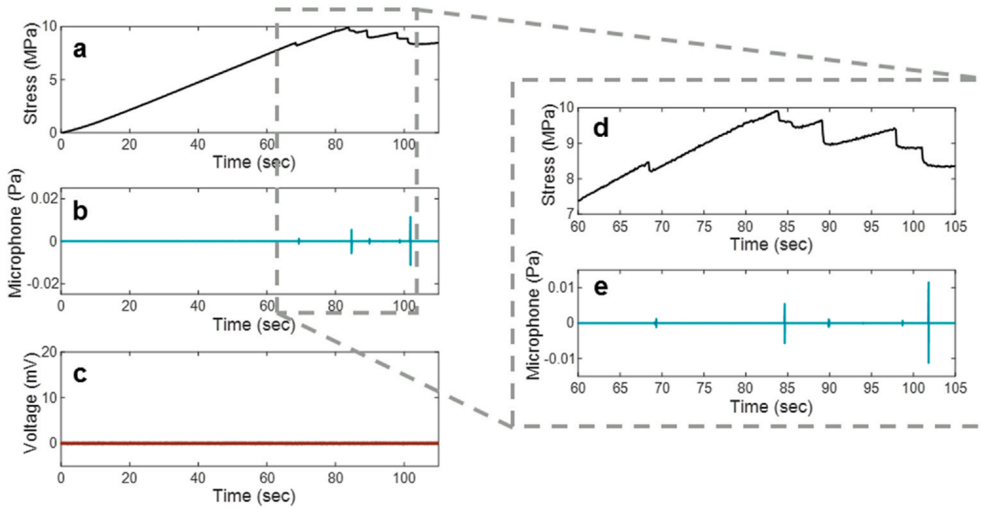

Fig. 3. (a) Applied stress, (b) microphone pressure reading, and (c) sample voltage for one representative neat sample during three-point bend testing. Magnified sections of the (d) applied stress and (e) microphone pressure reading to confirm damage occurrence.

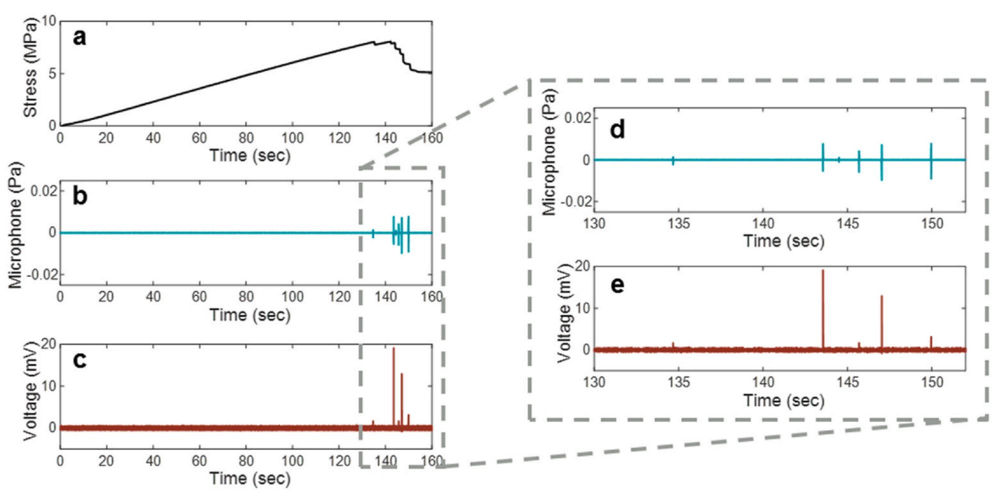

Fig. 4. (a) Applied stress, (b) microphone pressure reading, and (c) sample voltage for one representative sample containing DHF PVDF during three-point bend testing. Magnified sections of the (d) microphone pressure reading (e) sample voltage to confirm damage detection.

process result in sufficient electromechanical properties. As the sample is damaged via interlaminar delamination or fiber breaking during flexural loading, the DHF PVDF is perturbed resulting in a separation of charge. Thus, the voltage across the two electrodes surrounding the dielectric is observed to increase as a result. It is also worthwhile to note that the amplitude of the voltage emission is shown to correlate to the amplitude of the acoustic emission readings from the microphone, indicating that the damage severity, which has been shown previously to correlate to AET amplitude [41,65,66], is equally detectable by the multifunctional composite itself. In summary, the DHF PVDF is shown to add sensing functionality that was not observed from the neat samples, and the information collected is similar to that from the benchmark AET sensor. Thus, the need for an external structural health monitoring device or a system of discrete embedded sensors is eliminated by introducing an omnipresent ferroelectric sensing component fully integrated within the composite structure. Using this methodology, electrical measurements can be taken between any locations on the top and bottom surfaces of the composite in contrast to requiring electrical connections to embedded films.

3.3. *In-situ sensing during tensile testing*

In addition to flexural loading, both neat baseline samples and samples containing the same DHF PVDF prepreg were tested in a tensile testing configuration to further evaluate the ability of the DHF PVDF to detect various types of damage. Since the applied stress during tensile loading is much higher than that during flexural loading and the load cell is less sensitive to microdamage at such magnitudes, damage is not observed in the applied stress measurements prior to catastrophic failure. However, the same high frequency microphone which was shown to successfully detect damage during flexural loading was also used to detect acoustic emission output during tensile loading to confirm the occurrence of damage. The applied stress, microphone pressure reading, and voltage across the sample thickness for a representative neat composite sample are shown in Fig. 5a–c, respectively. As was observed during the flexural loading of a baseline sample, the microphone pressure reading (Fig. 5b) shows acoustic emission activity during the latter portion of the test (final ~30%). However, the voltage reading across the sample once again shows no measurable activity due to the lack of any inherent sensing component. At catastrophic failure, the voltage across the sample shows a small increase resulting from the complete failure of the sample leading to a rapid change in resistance and capacitance, as

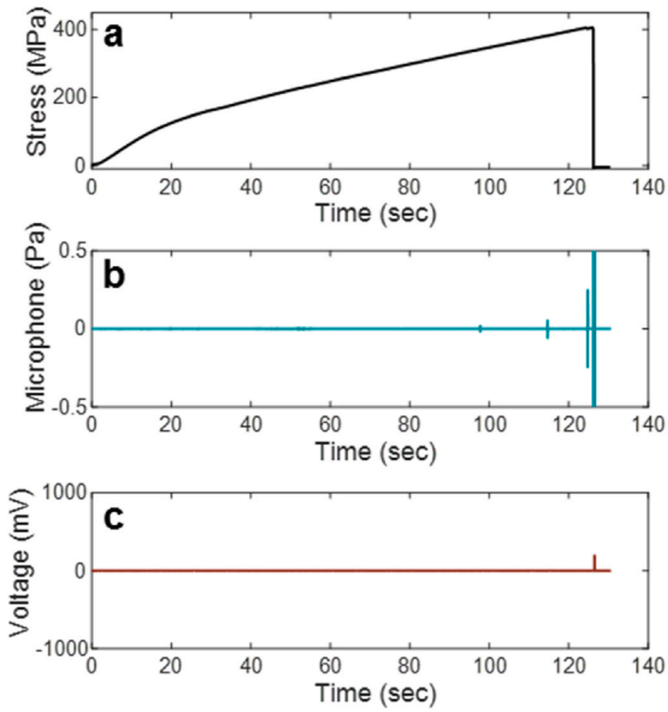

Fig. 5. (a) Applied stress, (b) microphone pressure reading, and (c) sample voltage for one representative neat sample during tensile testing.

well as disturbance to the wire leads attached to the surface of the sample that produces an artifact in the measurement. Thus, the baseline sample is incapable of sensing any damage prior to complete failure.

As was observed during the three-point bend testing, the composite samples containing DHF PVDF also showed a strong voltage response during tensile testing. Fig. 6a–c shows the applied stress, microphone pressure reading, and voltage emission across the sample for a representative DHF PVDF composite sample. Similar to what was observed during flexural loading, the sample shows a voltage emission correlating to acoustic emission readings from the high frequency microphone, which is particularly evident as the sample approaches complete failure. For greater clarity, the microphone pressure reading and voltage across the PVDF sample during a portion of the test is shown at higher magnification in Fig. 6d and e, respectively. As was discussed previously, the propagating waves detected by the microphone and the voltage emissions measured across the sample once again show correlation, not only in approximate time of occurrence, but in relative amplitude as well. This supports the assertion that the amplitude of the voltage emission, similar to AET measurements, corresponds to the significance of the damage. Prior AET work has shown that the AET amplitude increases with damage significance, with matrix cracking being the least, followed by fiber matrix debonding and interlaminar delamination, while fiber breakage results in the highest amplitude emission [41]. In addition to the evidence shown in Fig. 6, this phenomenologically holds true for multifunctional composites containing a piezoelectric component as well. While less significant damage such as matrix cracking results in only a small mechanical perturbation of the piezoelectric component, more significant damage such as delamination or fiber breakage results in a large mechanical change in strain, resulting in increased charge separation due to the direct piezoelectric effect, and thus a larger magnitude voltage emission measurement across the surrounding electrodes. This correlation is further discussed in prior works investigating piezoelectric ZnO nanowires for in-situ damage detection using the same methodology employed here [60].

To further analyze the response of the DHF PVDF hybrid composite, a closer examination of the response mechanism of both the microphone readings and the voltage measurements across the sample was completed. A single acoustic emission burst detected by the microphone and the corresponding voltage emission measured across the sample are shown in Fig. 7a and b, respectively. From Fig. 7a, the high frequency microphone functions as an AET sensor which detects the propagating waves resulting from damage. As damage occurs, a release in mechanical energy results in the propagation of an elastic wave that was detected by the microphone as a burst signal. In contrast, Fig. 7b shows the corresponding voltage response to the same damage incident. The composite containing DHF PVDF was designed and fabricated to possess the same fundamental functional components as a traditional piezoelectric sensor. As the composite experiences an internal change in strain, charge separation occurs and results in the rapid increase in the voltage measurement. This is followed by a discharge manifested by an exponential decay, which is characteristic of capacitive components. Therefore, the multifunctional composite acts as a capacitor that charges and discharges in response to a strain impulse resulting in the initial charge. This is similar to the response observed from samples containing ZnO rather than PVDF in the dielectric material between the electrodes, thus supporting the assertion that this voltage emission damage detection mechanism is characteristic of composites fabricated with inherent

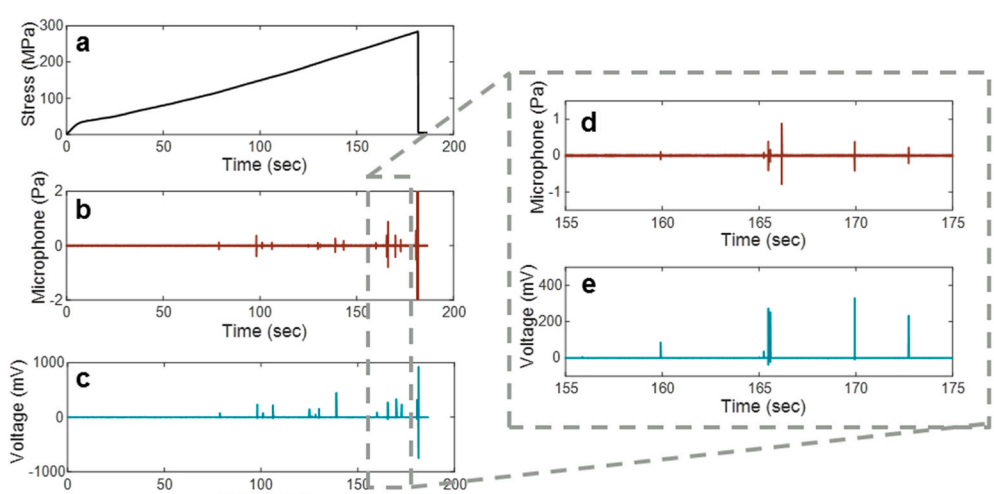

Fig. 6. (a) Applied stress, (b) microphone pressure reading, and (c) sample voltage for one representative sample containing DHF PVDF during tensile testing. Magnified sections of the (d) microphone pressure reading (e) sample voltage to confirm damage detection.

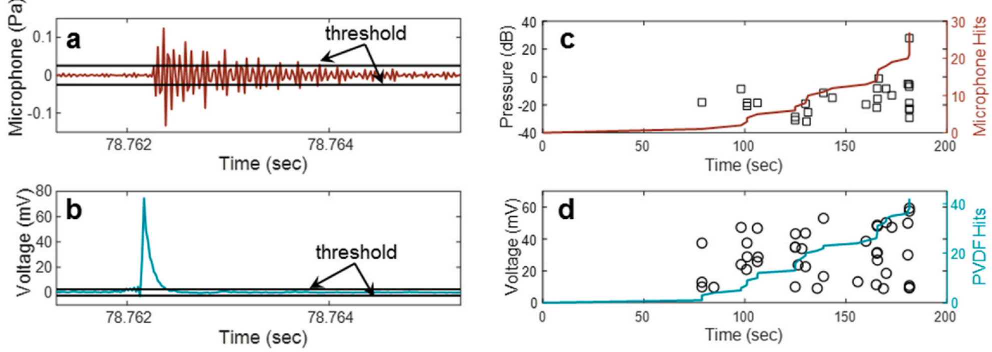

Fig. 7. Example of a "hit" indicating damage detection from (a) the AET microphone and (b) the PVDF composite. Detected hit amplitude (left) and cumulative number of hits (right) versus time for (c) the AET microphone and (d) the PVDF composite.

piezoelectric sensing functionality [60].

To further evaluate the occurrence of damage, a minimum threshold was defined for both the microphone reading and the voltage measurement. Each instance of an increase in the signal magnitude above the specified threshold is referred to as a "hit." In an effort to establish a fair comparison between damage detection methods, several requirements were met in determining the hit threshold for both the microphone and voltage measurements: (1) each burst signal recorded by the microphone was considered a single hit, (2) each hit was required to be separated by 5 ms to eliminate the counting of reflective waves by the microphone, (3) a root mean square (RMS) signal to noise ratio (SNR) was defined by calculating the RMS value of the hit amplitudes divided by the RMS value of the baseline noise, and (4) the threshold of both the microphone and voltage was adjusted until the RMS SNR was within 10 between the two measurements. Thus, the threshold accounted for differences between the baseline readings of each measurement and provided a fair comparison between the two measurements techniques to establish the effectiveness of the DHF PVDF against the widely accepted acoustic emission benchmark. The resulting RMS SNR values were calculated to be 1259 and 1252 for the microphone and voltage readings, respectively, which resulted in threshold magnitudes of approximately 25 mPa for the microphone reading and approximately 2.4 mV for the voltage reading. Using these defined thresholds, the amplitude of each hit and the cumulative number of hits versus time for both the microphone and voltage are shown in Fig. 7c and d, respectively. A visual examination of the data illustrates that the sample containing DHF PVDF shows comparable damage detection capabilities to the high frequency microphone in the approximate instance of occurrence, relative amplitude, and cumulative number of hits, indicating that the voltage emission method shows similar effectiveness to traditional AET. Therefore, voltage measurements taken directly from the composite allow for the tracking of the damage history of the composite for structural failure prediction and prevention purposes. However, unlike AET methods, the voltage emissions here are detected via the multifunctional composite itself, without any need for external sensors. Furthermore, the DHF PVDF is present throughout the entirety of the plane of the composite, therefore allowing for complete damage detection capabilities throughout the full area of the composite structure under investigation. To this end, it should also be noted that the woven carbon fabric comprising the top and bottom plies of the composite also serve as electrodes, which cover the plane of the composite, further supporting the omnipresent nature of the proposed sensing mechanism. It can also be noted that in practice, extensive baseline testing is used to determine an empirical threshold for AET. It is expected that a similar analysis would be completed for future widespread application of the novel piezoelectric prepreg discussed here, however, the threshold determined in this work was considered sufficient for an initial investigation to establish the functionality of the material in damage sensing.

4. Conclusions

The merit of this work is the investigation of a fully integrated alternative damage sensing mechanism to current methods that require the attachment of external or discrete sensors for in-situ SHM of fiber-reinforced composites. First, a thermally stable DHF PVDF prepreg was fabricated and characterized using FTIR. The ferroelectric prepreg was then used to fabricate a structural piezoelectric sensor by placing the insulating prepreg between carbon fiber fabrics which act as electrodes. As a result, the sensing capabilities are fully distributed throughout the composite, and the need for multiple embedded sensors is eliminated. Additionally, the structural integrity of the interlaminar region was found to be maintained through strategic placement of the DHF PVDF prepreg within the composite layup as confirmed through SBS testing. This composite was then subjected to flexural and tensile loading, during which it proved capable of sensing both the time of occurrence and relative significance of damage during both loading conditions, in a comparable manner to the employed benchmark AET sensor. The damage monitoring technique required no current input to the sample, and instead passively measured the voltage output of the sample. The cumulative processing of the passive measurements was then shown to be useful in the analysis of the damage history of the composite structure by tracking the cumulative number of hits. Therefore, multifunctional composites containing DHF PVDF provide a scalable, fully integrated, and omnipresent alternative to current AET sensing techniques, and can be used to detect early damage in-situ with the goal of increasing the safety and reliability of composite structures.

CRediT authorship contribution statement

LoriAnne Groo: Conceptualization, Investigation, Writing – original draft. **Daniel J. Inman:** Project administration, Methodology, Writing – review & editing. **Henry A. Sodano:** Conceptualization, Project administration, Methodology, Funding acquisition, Supervision, Writing – review & editing.

Declaration of competing interest

The authors declare that they have no known competing financial interests or personal relationships that could have appeared to influence the work reported in this paper.

Acknowledgements

This work was supported by the National Science Foundation Graduate Research Fellowship Program grant # DGE 1256260, National Science Foundation grant # CMMI-1762369 and # EFRI-1935216, and the Air Force Office of Scientific Research under grant # FA9550-16-1-0087.

Appendix A. Supplementary data

Supplementary data to this article can be found online at https://doi.org/10.1016/j.compscitech.2021.108982.

References

[1] P. Alander, L.V. Lassila, A. Tezvergil, P.K. Vallittu, Acoustic emission analysis of fiber-reinforced composite in flexural testing, Dent. Mater. 20 (4) (2004) 305–312.

[2] S. Barré, M.L. Benzeggagh, On the use of acoustic emission to investigate damage mechanisms in glass-fibre-reinforced polypropylene, Compos. Sci. Technol. 52 (3) (1994) 369–376.

[3] C. Barile, C. Casavola, G. Pappalettera, V.P. Kannan, Application of Different Acoustic Emission Descriptors in Damage Assessment of Fiber Reinforced Plastics: A Comprehensive Review, Engineering Fracture Mechanics, 2020, p. 107083.

[4] M.G. Sause, S. Schmitt, S. Kalafat, Failure load prediction for fiber-reinforced composites based on acoustic emission, Compos. Sci. Technol. 164 (2018) 24–33.

[5] C. Baron, K. Schulte, Electric Resistance Measurement for in Situ Determination of Fiber Failure in Carbon Fiber Reinforced Laminates, 1988.

[6] K. Schulte, C. Baron, Load and failure analyses of CFRP laminates by means of electrical resistivity measurements, Compos. Sci. Technol. 36 (1) (1989) 63–76.

[7] D.D.L. Chung, Structural health monitoring by electrical resistance measurement, Smart Mater. Struct. 10 (4) (2001) 624–636.

[8] A. Baltopoulos, N. Polydorides, L. Pambaguian, A. Vavouliotis, V. Kostopoulos, Exploiting carbon nanotube networks for damage assessment of fiber reinforced composites, Compos. B Eng. 76 (2015) 149–158.

[9] G.J. Gallo, E.T. Thostenson, Spatial damage detection in electrically anisotropic fiber-reinforced composites using carbon nanotube networks, Compos. Struct. 141 (2016) 14–23.

[10] G. Zhou, L. Sim, Damage detection and assessment in fibre-reinforced composite structures with embedded fibre optic sensors-review, Smart Mater. Struct. 11 (6) (2002) 925.

[11] C. Doyle, A. Martin, T. Liu, M. Wu, S. Hayes, P. Crosby, G. Powell, D. Brooks, G. Fernando, In-situ process and condition monitoring of advanced fibre-reinforced composite materials using optical fibre sensors, Smart Mater. Struct. 7 (2) (1998) 145.

[12] D. Wada, H. Igawa, M. Tamayama, T. Kasai, H. Arizono, H. Murayama, Flight demonstration of aircraft wing monitoring using optical fiber distributed sensing system, Smart Mater. Struct. 28 (5) (2019), 055007.

[13] H. Kwon, Y. Park, J.-H. Kim, C.-G. Kim, Embedded fiber Bragg grating sensor–based wing load monitoring system for composite aircraft, Struct. Health Monit. 18 (4) (2019) 1337–1351.

[14] X. Wang, X. Fu, D.D.L. Chung, Strain sensing using carbon fiber, J. Mater. Res. 14 (3) (2011) 790–802.

[15] S. Wang, D.D.L. Chung, Self-sensing of flexural strain and damage in carbon fiber polymer-matrix composite by electrical resistance measurement, Carbon 44 (13) (2006) 2739–2751.

[16] J.C. Abry, S. Bochard, A. Chateauminois, M. Salvia, G. Giraud, In situ detection of damage in CFRP laminates by electrical resistance measurements, Compos. Sci. Technol. 59 (6) (1999) 925–935.

[17] J. Wen, Z. Xia, F. Choy, Damage detection of carbon fiber reinforced polymer composites via electrical resistance measurement, Compos. B Eng. 42 (1) (2011) 77–86.

[18] H. Mahmood, L. Vanzetti, M. Bersani, A. Pegoretti, Mechanical properties and strain monitoring of glass-epoxy composites with graphene-coated fibers, Compos. Appl. Sci. Manuf. 107 (2018) 112–123.

[19] R. Balaji, M. Sasikumar, Graphene based strain and damage prediction system for polymer composites, Compos. Appl. Sci. Manuf. 103 (2017) 48–59.

[20] L. Gao, E.T. Thostenson, Z. Zhang, T.-W. Chou, Sensing of damage mechanisms in fiber-reinforced composites under cyclic loading using carbon nanotubes, Adv. Funct. Mater. 19 (1) (2009) 123–130.

[21] S.-l. Gao, R.-C. Zhuang, J. Zhang, J.-W. Liu, E. Mäder, Glass fibers with carbon nanotube networks as multifunctional sensors, Adv. Funct. Mater. 20 (12) (2010) 1885–1893.

[22] N.D. Alexopoulos, C. Bartholome, P. Poulin, Z. Marioli-Riga, Structural health monitoring of glass fiber reinforced composites using embedded carbon nanotube (CNT) fibers, Compos. Sci. Technol. 70 (2) (2010) 260–271.

[23] H. Zhang, E. Bilotti, T. Peijs, The use of carbon nanotubes for damage sensing and structural health monitoring in laminated composites: a review, Nanocomposites 1 (4) (2015) 167–184.

[24] A. Godara, L. Gorbatikh, G. Kalinka, A. Warrier, O. Rochez, L. Mezzo, F. Luizi, A. W. van Vuure, S.V. Lomov, I. Verpoest, Interfacial shear strength of a glass fiber/epoxy bonding in composites modified with carbon nanotubes, Compos. Sci. Technol. 70 (9) (2010) 1346–1352.

[25] L. Gao, T.-W. Chou, E.T. Thostenson, Z. Zhang, M. Coulaud, In situ sensing of impact damage in epoxy/glass fiber composites using percolating carbon nanotube networks, Carbon 49 (10) (2011) 3382–3385.

[26] M. Tehrani, A. Boroujeni, T. Hartman, T. Haugh, S. Case, M. Al-Haik, Mechanical characterization and impact damage assessment of a woven carbon fiber reinforced carbon nanotube–epoxy composite, Compos. Sci. Technol. 75 (2013) 42–48.

[27] F.H. Gojny, M.H.G. Wichmann, U. Köpke, B. Fiedler, K. Schulte, Carbon nanotube-reinforced epoxy-composites: enhanced stiffness and fracture toughness at low nanotube content, Compos. Sci. Technol. 64 (15) (2004) 2363–2371.

[28] T. Liu, M. Wu, Y. Rao, D.A. Jackson, G.F. Fernando, A multiplexed optical fibre-based extrinsic Fabry-Perot sensor system for in-situ strain monitoring in composites, Smart Mater. Struct. 7 (4) (1998) 550.

[29] S. Minakuchi, In situ characterization of direction-dependent cure-induced shrinkage in thermoset composite laminates with fiber-optic sensors embedded in through-thickness and in-plane directions, J. Compos. Mater. 49 (9) (2015) 1021–1034.

[30] G. Kister, B. Ralph, G.F. Fernando, Damage detection in glass fibre-reinforced plastic composites using self-sensing E-glass fibres, Smart Mater. Struct. 13 (5) (2004) 1166.

[31] K. Kuang, W. Cantwell, Use of conventional optical fibers and fiber Bragg gratings for damage detection in advanced composite structures: a review, Appl. Mech. Rev. 56 (5) (2003) 493–513.

[32] I.M. Perez, H. Cui, E. Udd, Acoustic Emission Detection Using Fiber Bragg Gratings, Smart Structures and Materials 2001: Sensory Phenomena and Measurement Instrumentation for Smart Structures and Materials, International Society for Optics and Photonics, 2001, pp. 209–215.

[33] H. Tsuda, E. Sato, T. Nakajima, H. Nakamura, T. Arakawa, H. Shiono, M. Minato, H. Kurabayashi, A. Sato, Acoustic emission measurement using a strain-insensitive fiber Bragg grating sensor under varying load conditions, Opt Lett. 34 (19) (2009) 2942–2944.

[34] Q. Wu, F. Yu, Y. Okabe, S. Kobayashi, Application of a novel optical fiber sensor to detection of acoustic emissions by various damages in CFRP laminates, Smart Mater. Struct. 24 (1) (2014), 015011.

[35] R. Hadzic, S. John, I. Herszberg, Structural integrity analysis of embedded optical fibres in composite structures, Compos. Struct. 47 (1) (1999) 759–765.

[36] K. Shivakumar, L. Emmanwori, Mechanics of failure of composite laminates with an embedded fiber optic sensor, J. Compos. Mater. 38 (8) (2004) 669–680.

[37] K. Komai, K. Minoshima, T. Shibutani, Investigations of the fracture mechanism of carbon/epoxy composites by AE signal analyses, JSME international journal. Ser. 1, Solid mechanics, strength of materials 34 (3) (1991) 381–388.

[38] P.J. de Groot, P.A.M. Wijnen, R.B.F. Janssen, Real-time frequency determination of acoustic emission for different fracture mechanisms in carbon/epoxy composites, Compos. Sci. Technol. 55 (4) (1995) 405–412.

[39] J.Q. Huang, 2 - non-destructive evaluation (NDE) of composites: acoustic emission (AE), in: V.M. Karbhari (Ed.), Non-Destructive Evaluation (NDE) of Polymer Matrix Composites, Woodhead Publishing2013, pp. 12-32.

[40] S. Masmoudi, A. El Mahi, S. Turki, Fatigue behaviour and structural health monitoring by acoustic emission of E-glass/epoxy laminates with piezoelectric implant, Appl. Acoust. 108 (2016) 50–58.

[41] H. Bar, M. Bhat, C. Murthy, Parametric analysis of acoustic emission signals for evaluating damage in composites using a PVDF film sensor, J. Nondestr. Eval. 24 (4) (2005) 121–134.

[42] H. Bar, M. Bhat, C. Murthy, Identification of failure modes in GFRP using PVDF sensors: ANN approach, Compos. Struct. 65 (2) (2004) 231–237.

[43] J.-M. Park, J.-W. Kong, D.-S. Kim, D.-J. Yoon, Nondestructive damage detection and interfacial evaluation of single-fibers/epoxy composites using PZT, PVDF and P (VDF-TrFE) copolymer sensors, Compos. Sci. Technol. 65 (2) (2005) 241–256.

[44] A. Jain, S. Minajagi, E. Dange, S.U. Bhover, Y. Dharanendra, Impact and Acoustic Emission Performance of Polyvinylidene Fluoride Sensor Embedded in Glass Fiber-Reinforced Polymer Composite Structure, Polymers and Polymer Composites, 2020, 0967391120915334.

[45] P. Ueberschlag, PVDF Piezoelectric Polymer, Sensor review, 2001.

[46] W.-Y. Chang, C.-H. Chu, Y.-C. Lin, A flexible piezoelectric sensor for microfluidic applications using polyvinylidene fluoride, IEEE Sensor. J. 8 (5) (2008) 495–500.

[47] J.-H. Bae, S.-H. Chang, Characterization of an electroactive polymer (PVDF-TrFE) film-type sensor for health monitoring of composite structures, Compos. Struct. 131 (2015) 1090–1098.

[48] H. Tzou, M. Gadre, Theoretical analysis of a multi-layered thin shell coupled with piezoelectric shell actuators for distributed vibration controls, J. Sound Vib. 132 (3) (1989) 433–450.

[49] Y. Fu, E.C. Harvey, M.K. Ghantasala, G.M. Spinks, Design, fabrication and testing of piezoelectric polymer PVDF microactuators, Smart Mater. Struct. 15 (1) (2005) S141.

[50] R. Hasegawa, Y. Takahashi, Y. Chatani, H. Tadokoro, Crystal structures of three crystalline forms of poly (vinylidene fluoride), Polym. J. 3 (5) (1972) 600–610.

[51] E. Fukada, T. Furukawa, Piezoelectricity and ferroelectricity in polyvinylidene fluoride, Ultrasonics 19 (1) (1981) 31–39.

[52] M.G. Broadhurst, G.T. Davis, J.E. McKinney, R.E. Collins, Piezoelectricity and pyroelectricity in polyvinylidene fluoride—a model, J. Appl. Phys. 49 (10) (1978) 4992–4997.

[53] R. Gregorio, E. Ueno, Effect of crystalline phase, orientation and temperature on the dielectric properties of poly (vinylidene fluoride)(PVDF), J. Mater. Sci. 34 (18) (1999) 4489–4500.

[54] K. Matsushige, K. Nagata, S. Imada, T. Takemura, The II-I crystal transformation of poly(vinylidene fluoride) under tensile and compressional stresses, Polymer 21 (12) (1980) 1391–1397.

[55] C.-h. Du, B.-K. Zhu, Y.-Y. Xu, Effects of stretching on crystalline phase structure and morphology of hard elastic PVDF fibers, J. Appl. Polym. Sci. 104 (4) (2007) 2254–2259.

[56] V. Sencadas, R. Gregorio Jr., S. Lanceros-Méndez, α to β phase transformation and microestructural changes of PVDF films induced by uniaxial stretch, J. Macromol. Sci. 48 (3) (2009) 514–525.

[57] L.L. Blyler, G.E. Johnson, N.M. Hylton, Characterization of biaxially-oriented polyvinylidene fluoride-film for transducer applications, Ferroelectrics 28 (1) (1980) 303–306.

[58] G.E. Johnson, L.L. Blyler, G.R. Crane, C. Gieniewski, Thermal piezoelectric stability of poled uniaxially-and biaxially-oriented poly(vinylidene fluoride, Ferroelectrics 32 (1) (1981) 43–47.
[59] J. Lin, M.H. Malakooti, H.A. Sodano, Thermally stable poly (vinylidene fluoride) for high-performance printable piezoelectric devices, ACS Appl. Mater. Interfaces 12 (19) (2020) 21871–21882.
[60] L. Groo, D.J. Inman, H.A. Sodano, In situ damage detection for fiber-reinforced composites using integrated zinc oxide nanowires, Adv. Funct. Mater. 28 (35) (2018) 1802846.
[61] J. Lin, S.H. Bang, M.H. Malakooti, H.A. Sodano, Isolation of aramid nanofibers for high strength and toughness polymer nanocomposites, ACS Appl. Mater. Interfaces 9 (12) (2017) 11167–11175.
[62] M.H. Malakooti, B.A. Patterson, H.-S. Hwang, H.A. Sodano, ZnO nanowire interfaces for high strength multifunctional composites with embedded energy harvesting, Energy Environ. Sci. 9 (2) (2016) 634–643.
[63] X. Cai, T. Lei, D. Sun, L. Lin, A critical analysis of the α, β and γ phases in poly (vinylidene fluoride) using FTIR, RSC Adv. 7 (25) (2017) 15382–15389.
[64] T. Krause, S. Preihs, J. Ostermann, in: Acoustic Emission Damage Detection for Wind Turbine Rotor Blades Using Airborne Sound, Proceedings of 10th International Workshop on Structural Health Monitoring, IWSHM), 2015.
[65] N. Chandarana, D.M. Sanchez, C. Soutis, M. Gresil, Early damage detection in composites during fabrication and mechanical testing, Materials 10 (7) (2017) 685.
[66] M. Assarar, D. Scida, W. Zouari, E.H. Saidane, R. Ayad, Acoustic emission characterization of damage in short hemp-fiber-reinforced polypropylene composites, Polym. Compos. 37 (4) (2016) 1101–1112.